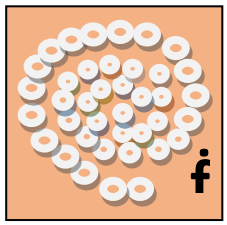

International Journal of Mathematical Analysis and Modelling

(Formerly Journal of the Nigerian Society for Mathematical Biology)

Volume 7 Issue 2, 2024

ISSN (Print): 2682 - 5694
ISSN (Online): 2682 – 5708
www.tnsmb.org

Laplace-Adomian Decomposition method for solving fractional-order mathematical model of Monkeypox transmission dynamics

B.C. Agbata[*], W. Obeng-Denteh[†], D.F. Agbebaku[‡§], M.M. Shior[**], D.J. Yahaya[††] and A.Y. Danjuma[‡‡]

Abstract

In this study, we developed a model to understand and predict the spread of Monkeypox among humans and rodents, both of which are important in the disease's transmission. Our model categorized the human population into six groups: susceptible individuals who have not been exposed, exposed individuals who have encountered the virus, infected individuals, quarantined individuals, those receiving treatment, and those who have recovered. For rodents, we considered three groups: susceptible, exposed, and infected animals, as they also play a key role in spreading Monkeypox. To explore how different control measures could impact the spread of the disease, we used a mathematical approach known as the Laplace Adomian Decomposition Method (LADM) to get an approximate solution to the model. This allows us to estimate the outcomes of various strategies in managing the disease. Our findings shed light on how actions like quarantining, treating infected individuals, and reducing the number of susceptible rodents can work together to slow or stop the spread of Monkeypox. This model gives public health officials a clearer picture of where to focus efforts to prevent outbreaks and protect communities.

Keywords and phrases: numerical methods; human-rodent interactions; mathematical epidemiology; series solution; numerical simulations

[*] Department of Mathematics and Statistics, Confluence University of Science and Technology, Osara, Nigeria.
[†] Department of Mathematics, Kwame Nkrumah University of Science and Technology, Kumasi, Ghana.
[‡] Corresponding author E-mail: dennis.agbebaku@unn.edu.ng
[§] Department of Mathematics, University of Nigeria, Nsukka
[**] Department of Mathematics/ Computer Science, Benue State University Makurdi, Nigeria
[††] Department of Mathematics and Statistics, Confluence University of Science and Technology, Osara, Nigeria.
[‡‡] Department of Actuarial Science, Confluence University of Science and Technology, Osara, Nigeria.

1 Introduction

Monkeypox has re-emerged as a global public health concern, shifting from sporadic outbreaks in endemic regions of Central and West Africa to a worldwide spread. The recent outbreak was declared a public health emergency of international concern by the World Health Organization (WHO) in July 2022 [1] after cases rapidly spread across North America, Europe, and other regions [3]. This change in monkeypox's epidemiology has underscored the urgent need for enhanced surveillance and understanding of transmission, especially as the virus increasingly affects diverse populations outside historically affected areas [1,2]. Monkeypox is caused by the Monkeypox virus (MPXV), a member of the Orthopoxvirus genus, and it is closely related to the smallpox virus. MPXV can transmit through direct contact with bodily fluids, respiratory droplets, or contaminated objects. Unlike in previous outbreaks, recent studies suggest transmission through close, often sexual contact, especially among men who have sex with men (MSM), though the virus remains capable of infecting anyone [2,3]. This shift in transmission patterns has led public health agencies to prioritize community education and risk reduction strategies, especially for vulnerable groups. The clinical presentation of monkeypox typically includes fever, rash, lymphadenopathy, and muscle aches. The incubation period ranges from 5 to 21 days, with symptoms lasting two to four weeks. Unlike smallpox, monkeypox typically causes a milder disease, but it can still lead to severe complications, particularly in immunocompromised individuals [3]. A recent study highlighted that those with untreated HIV infection or weakened immune systems are at greater risk of severe illness and mortality if infected with monkeypox [1,3]. To control the spread of monkeypox, health authorities have expanded diagnostic and testing capabilities. For instance, the U.S. Centers for Disease Control and Prevention (CDC) increased testing capacities significantly to accommodate the growing number of cases in 2022. Vaccination campaigns using the JYNNEOS vaccine, initially stockpiled for smallpox, have also been implemented as a preventive measure, especially for high-risk groups [2] . Additionally, tecovirimat (Tpoxx) is available under expanded access protocols as a treatment option, particularly for severe cases [2,3]. The resurgence of Monkeypox highlights the interconnectedness of global health and the need for preparedness. This recent outbreak underscores the importance of international collaboration in epidemiological research, timely surveillance, and robust public health response strategies. By improving diagnostic and treatment options, expanding access to vaccines, and implementing targeted interventions, health authorities aim to prevent future outbreaks and manage those at risk effectively [2,3].

The Laplace Adomian Decomposition Method (LADM) is a powerful analytical technique used to solve complex differential equations commonly encountered in mathematical modeling, including epidemiological studies. LADM combines the Laplace transform with Adomian Decomposition to break down differential equations into a series of manageable sub-problems. This hybrid approach leverages the Laplace transform's ability to simplify differential equations and Adomian's method of decomposing nonlinear terms, allowing for effective solutions in systems that are otherwise challenging to solve analytically [7,8]. LADM's adaptability to various boundary conditions and its

ability to handle nonlinear equations without requiring linearization make it a suitable choice for modeling infectious disease dynamics, such as monkeypox.

One of the main advantages of using LADM in monkeypox modeling is its effectiveness in obtaining approximate solutions that converge rapidly, often without the need for iterative approximation, as seen in traditional numerical methods. This characteristic is particularly beneficial in epidemiological modeling, where accurate, timely predictions of disease spread and control measures are crucial. For example, LADM allows researchers to explore various compartments in monkeypox transmission, such as susceptible, exposed, infected, and recovered populations, while efficiently estimating the impact of intervention strategies [5, 6]. By providing explicit, analytical expressions for these population compartments over time, LADM enhances the accuracy of disease models and aids in better understanding and predicting the dynamics of infectious diseases like monkeypox.LADM also supports sensitivity analysis, which assesses how changes in model parameters—such as transmission and recovery rates—impact the overall system dynamics. This feature is essential in infectious disease research, where understanding parameter sensitivity helps identify which factors are most influential in controlling outbreaks [4]. In monkeypox modeling, LADM's capacity for parameter sensitivity analysis aids in evaluating the effectiveness of public health interventions, such as vaccination and quarantine measures. Overall, LADM's combination of flexibility, accuracy, and computational efficiency makes it an invaluable tool in developing reliable epidemiological models that can inform and optimize strategies for disease control.

Mathematical modeling is a fundamental tool in scientific research for understanding and predicting complex systems across disciplines, particularly in epidemiology, where it plays a critical role in studying disease dynamics. Models use mathematical equations to represent real-world processes, allowing researchers to simulate and analyze the behavior of systems under various conditions [9]. In infectious disease modeling, for example, compartmental models like SIR (Susceptible, Infected, Recovered) and SEIR (Susceptible, Exposed, Infected, Recovered) categorize populations into compartments that describe disease progression stages. These models help estimate parameters like transmission and recovery rates, enabling scientists to assess the potential impact of public health interventions [10]. Additionally, mathematical models support decision-making in public health by providing insights into outbreak control, vaccine distribution, and policy effects. Recent advancements in modeling methods, including stochastic and agent-based models, have further enhanced their accuracy and applicability to real-world scenarios, emphasizing their importance in epidemiology and beyond [11].

Recent researchers have focused on a variety of mathematical models to assess monkeypox interventions, estimate transmission dynamics, and predict spread patterns across different conditions. [12] developed a stochastic compartmental model, separating populations into Susceptible, Exposed, Infectious, and Recovered (SEIR) categories, to estimate the reproduction number of monkeypox during the 2022 outbreak in non-endemic countries. Their findings highlighted that regions with dense populations and high mobility had higher reproduction numbers, underlining the impact of early

interventions like quarantine and isolation. [13] applied a compartmental model to evaluate vaccination strategies in the UK's 2022 outbreak, emphasizing that even with limited vaccine supplies, targeting high-risk populations could substantially reduce transmission rates. Their model also pointed to the significance of timely vaccine distribution and rapid case detection.

[14] presented a deterministic model simulating monkeypox transmission in West Africa, incorporating both zoonotic and human-to-human transmission. Their analysis indicated that human transmission plays an increasing role, especially in urban settings, and recommended enhanced public health surveillance. [15] introduced a dynamic model that examined how behavior changes, such as social distancing and improved hygiene, affect monkeypox spread. The study showed that these behavioral shifts reduce the effective reproduction number, highlighting the importance of public health campaigns during outbreaks. Lastly, [16] developed a network-based model to simulate monkeypox spread in social and sexual networks, focusing on the heterogeneity of contact patterns within certain communities. Their research emphasized that interventions like vaccination are particularly effective in high-contact subpopulations, such as MSM (men who have sex with men), which are more vulnerable to outbreaks.

The novelty of this study lies in its dual-host modeling approach, which simultaneously considers both human and rodent populations to capture the complex transmission dynamics of Monkeypox—a factor often overlooked in previous models that focus primarily on human-to-human spread. By incorporating distinct epidemiological compartments for both species, this study provides a more comprehensive framework for understanding the role of zoonotic reservoirs in sustaining outbreaks. Furthermore, the use of the Laplace Adomian Decomposition Method (LADM) to obtain approximate solutions introduces an innovative mathematical approach that enhances the model's analytical tractability, allowing for more efficient evaluation of disease control strategies. Unlike conventional numerical methods, LADM provides a semi-analytical solution that improves accuracy and computational efficiency, making it particularly valuable for real-time policy assessments. Additionally, this study uniquely bridges theoretical epidemiology with practical public health interventions by evaluating the synergistic effects of multiple control measures, such as quarantining, treatment, and rodent population management, offering actionable insights for outbreak prevention. By integrating mathematical modeling with applied disease control strategies, this research presents a novel and impactful contribution to Monkeypox epidemiology, equipping policymakers with targeted recommendations to mitigate future outbreaks.

2 Materials and methods

We develop a deterministic compartmental model on the transmission dynamics of Monkeypox consisting of human and rodent population [22]. The human population comprises of six epidemiological groups, Susceptible humans $S_h(t)$, exposed humans $E_h(t)$, infected humans $I_h(t)$, quarantined humans $Q_h(t),$, treated humans $T_h(t)$ and recovered humans $R_h(t)$. The rodent

population is subdivided into three compartments namely: Susceptible rodents $S_r(t)$, exposed humans $E_r(t)$, infected rodents $I_r(t)$. The recruitment rate of human population is given as Λ_h and β_{rh} is the effective contact rate with the probability of human been infected with Monkeypox virus due to contact with infected rodent. β_{hh} denotes effective contact rate and the probability human been infected with monkeypox virus due to contact with infectious human and ω_h is the progression rate from exposed human to highly infected human whereas the treatment rate of infected humans is ρ_h and the recovery rate of treated humans is τ_h. θ_h is the quarantined rate of exposed humans whereas γ_h is the rate at which quarantined humans become susceptible and the recovery rate of quarantined humans is ψ_h. Natural death occurs in the humans and rodents' population at the rates μ_h and μ_r respectively. The infected humans and rodents' population decrease by the disease induced death rates δ_h and δ_r respectively. Λ_r is rodents' recruitment rate and β_{rr} is the effective contact rate with the probability of rodent been infected per contact rate with already infected rodent. ω_r is the progression rate from exposed rodent population to highly infectious rodent population and is immunity loss rate. The transition from one epidemiological compartment to another is illustrated in figure 1 below.

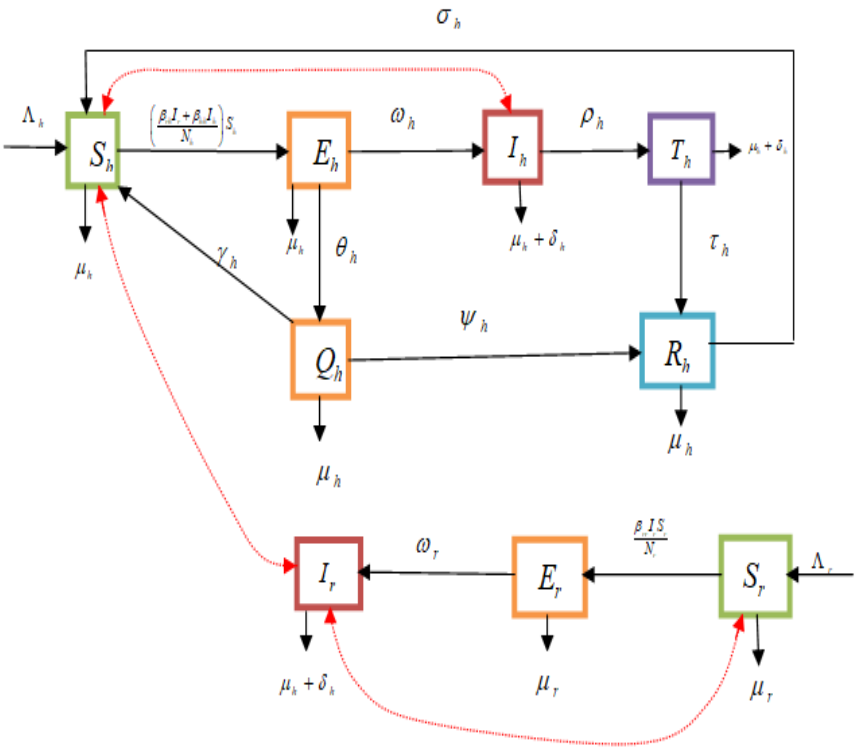

Figure 1. Schematic diagram for the model [22] .

Table 1. Description of variables and parameters

Variables	Description
$S_h(t)$	Susceptible human
$E_h(t)$	Exposed human
$Q_h(t)$	Isolated/quarantined human
$I_h(t)$	Infected human
$T_h(t)$	Treated human
$R_h(t)$	Recovered human
$S_r(t)$	Susceptible rodent
$E_r(t)$	Exposed rodent
$I_r(t)$	Infected rodents
Λ_h	Human recruitment rate
β_{rh}	Rodent contact rate to human
β_{hh}	Human to human contact rate
β_{rr}	Rodent to rodent to contact rate
ω_h	Progression rate from exposed human to infected human
ρ_h	Human treatment rate
θ_h	Quarantined rate of exposed humans
γ_h	Quarantined rate of susceptible humans
ψ_h	Recovery rate of quarantined individual
τ_h	Recovery rate of infected human
γ_h	Rate at which quarantined human become susceptible
σ_h	Immunity loss rate for human population
δ_h	Disease induced death rate for human
δ_r	Disease induce death rate for rodents
μ_h	Natural death rate for human
μ_r	Natural death rate for rodents
ω_r	Progression rate from exposed rodent to infected rodent

2.1 Model equations

The model is governed by the following set of differential equations.

$$\frac{dS_h}{dt} = \Lambda_h + \sigma_h R_h + \alpha_h Q_h - \frac{(\beta_{rh} \mathrm{I}_r + \beta_{hh} \mathrm{I}_h)\mathrm{S}_h}{N_h} - \mu_h S_h$$

$$\frac{dE_h}{dt} = \frac{(\beta_{rh} \mathrm{I}_r + \beta_{hh} \mathrm{I}_h)\mathrm{S}_h}{N_h} - (\omega_h + \theta_h + \mu_h)\mathrm{E}_h$$

$$\frac{dI_h}{dt} = \omega_h E_h - (\rho_h + \delta_h + \mu_h) I_h$$

$$\frac{dQ_h}{dt} = \theta_h E_h - (\alpha_h + \psi_h + \mu_h)\mathrm{Q}_h \qquad (1)$$

$$\frac{dT_h}{dt} = \rho_h I_h - (\tau_h + \delta_h + \mu_h)\mathrm{T}_h$$

$$\frac{dR_h}{dt} = \psi_h Q_h + \tau_h T_h - (\sigma_h + \mu_h)\mathrm{R}_h$$

$$\frac{dS_r}{dt} = \Lambda_r - \frac{\beta_{rr} I_r S_r}{N_r} - \mu_r \mathrm{S}_r$$

$$\frac{dE_r}{dt} = \frac{\beta_{rr} I_r S_r}{N_r} - (\omega_r + \mu_r)\mathrm{E}_r$$

$$\frac{dI_r}{dt} = \omega_r \mathrm{E}_r - (\delta_r + \mu_r)\mathrm{I}_r \quad \text{P7}$$

where $\lambda_h = \frac{(\beta_{rh} I_r + \beta_{hh} I_h)}{N_h}$, $\lambda_r = \frac{\beta_{rr} I_r}{N_r}$

2.1.1 Model Analysis

Total human population,

$N_h = S_h + E_h + I_h + \mathrm{Q}_h + T_h + R_h$

The differential equation yields

$\frac{dN_h}{dt} = \Lambda_h - \delta_h I_h - \mu_h N_h$

Total rodent population,

$N_r = S_r + E_r + I_r$

The differential equation also gives

$\frac{dN_r}{dt} = \Lambda_r - (\mu_r + \Lambda_r) N_r$

Lemma 1

Let $(S_h, E_h, I_h, Q_h, T_h, R_h, S_r, E_r, I_r)$ be the solution of the model (1) with initial conditions in a epidemiological feasible region $D = D_h \times D_r$ with [22]:

$$D_h = S_h, E_h, I_h, Q_h, T_h, R_h \in R_+^6 : N_h \leq \frac{\Lambda_h}{\mu_h}$$

and

$$D_r = S_r, E_r, I_r \in R_+^3 : N_r \leq \frac{\Lambda_r}{\mu_r}$$

Then D is non-negative invariant

From the result of [23], we obtain

$$0 \leq N_h(t) \leq N_h(0) e^{-\mu_h(t)} + \frac{\Lambda_h}{\mu_h}\left(1 - e^{-\mu_h(t)}\right)$$

and

$$0\, N_r(t) \leq N_r(0) e^{-(\mu_r + \Lambda_r)t} + \frac{\Lambda_h}{\mu_h}\left(1 - e^{-(\mu_r + \Lambda_r)t}\right)$$

Therefore, the set D is positively invariant for all t

Asymptotic Stability of the Disease-Free Equilibrium of the Monkeypox Model

The disease-free equilibrium is given below [22]

$$\eta_0 = \left\{S_h^*, E_h^*, I_h^*, Q_h^*, T_h^*, R_h^*, S_r^*, E_r^*, I_r^*\right\} = \left\{\frac{\Lambda_h}{\mu_h}, 0, 0, 0, 0, 0, \frac{\Lambda_r}{\mu_r}, 0, 0\right\}$$

Basic Reproduction Number

In this article, R_0 is obtained using the next generation operator method on the dynamic system (1), as detailed below [22].

Hence, it follows that

$R_0 = \rho\left(FV^{-1}\right)$ where ρ is the dominant eigenvalue of FV^{-1}

$$F=\begin{bmatrix} 0 & \beta_{hh} & 0 & 0 & 0 & \beta_{rh} \\ 0 & 0 & 0 & 0 & 0 & 0 \\ 0 & 0 & 0 & 0 & 0 & 0 \\ 0 & 0 & 0 & 0 & 0 & 0 \\ 0 & 0 & 0 & 0 & 0 & \beta_{rr} \\ 0 & 0 & 0 & 0 & 0 & 0 \end{bmatrix}, V=\begin{bmatrix} P_1 & 0 & 0 & 0 & 0 & 0 \\ -\omega_h & P_2 & 0 & 0 & 0 & 0 \\ \theta_h & 0 & P_3 & 0 & 0 & 0 \\ 0 & -\rho_h & 0 & P_4 & 0 & 0 \\ 0 & 0 & 0 & 0 & P_6 & 0 \\ 0 & 0 & 0 & 0 & -\omega_t & P_7 \end{bmatrix}$$

$$J=\begin{bmatrix} \frac{\beta_{hh}\omega_h}{P_2P_1} & \frac{\beta_{hh}}{P_2} & 0 & 0 & \frac{\beta_{rh}\omega_r}{P_6P_7} & \frac{\beta_{rh}}{P_7} \\ 0 & 0 & 0 & 0 & 0 & 0 \\ 0 & 0 & 0 & 0 & 0 & 0 \\ 0 & 0 & 0 & 0 & 0 & 0 \\ 0 & 0 & 0 & 0 & \frac{\beta_{rr}\omega_r}{P_6P_7} & \frac{\beta_{rr}}{P_7} \\ 0 & 0 & 0 & 0 & 0 & 0 \end{bmatrix}$$

The eigenvalues of FV^{-1} are

$$R_0^r=\frac{\beta_{rr}\omega_r}{P_6P_7}$$

$$R_0^h=\frac{\beta_{hh}\omega_h}{P_2P_1}$$

$$R_0=\left(R_0^h,R_0^r\right)$$

Jacobian Matrix (LAS)

$$J=\begin{bmatrix} \frac{\beta_{hh}\omega_h}{P_2P_1} & \frac{\beta_{hh}}{P_2} & 0 & 0 & \frac{\beta_{rh}\omega_r}{P_6P_7} & \frac{\beta_{rh}}{P_7} \\ 0 & 0 & 0 & 0 & 0 & 0 \\ 0 & 0 & 0 & 0 & 0 & 0 \\ 0 & 0 & 0 & 0 & 0 & 0 \\ 0 & 0 & 0 & 0 & \frac{\beta_{rr}\omega_r}{P_6P_7} & \frac{\beta_{rr}}{P_7} \\ 0 & 0 & 0 & 0 & 0 & 0 \end{bmatrix}$$

The reduced Jacobian matrix becomes

$$J_1=\begin{bmatrix} -P_1 & \beta_{hh} & 0 & \beta_{rh} \\ \omega_h & -P_2 & 0 & 0 \\ 0 & 0 & -P_6 & \beta_{rr} \\ 0 & 0 & \omega_r & -P_7 \end{bmatrix}$$

The characteristic polynomial becomes

$$\lambda^4+\left(P_7+P_6+P_2+P_1\right)\lambda^3+\left(P_2P_1+P_6P_1+P_7P_1+P_6P_2+P_7P_2+P_7P_6-\beta_{hh}\omega_h-\omega_r\beta_{rr}\right)\lambda^2$$
$$+\left(P_1P_2P_6+P_1P_2P_7+P_1P_6P_7-\omega_r\beta_{rr}P_1+P_2P_6P_7-\omega_r\beta_{rr}P_2-P_6\beta_{hh}\omega_h-P_7\beta_{hh}\omega_h\right)\lambda$$
$$+P_1P2\left(1-R_0^r\right)+P_6P_7\left(1-R_0^h\right)$$

Applying the Routh Hurwitz criterion, we observe that the DFE is locally asymptotically stable.

$P_1=(\omega_h+\theta_h+\mu_h)$ $P_2=(\rho_h+\delta_h+\mu_h)$ $P_3=(\alpha_h+\psi_h+\mu_h)$ $P_4=(\tau_h+\delta_h+\mu_h)$ $P_5=(\sigma_h+\mu_h)$

$P_6=(\omega_r+\mu_r)$ $P_7=(\delta_r+\mu_r)$.

Global Asymptotic Stability of the Disease Free Equilibrium Point of the Monkeypox Model.

To investigate the global stability of the disease free equilibrium, we use the technique implemented by Castillo-Chavez and song [22, 24].

To do this, we write the equation in the uninfected class as

$$\frac{dX}{dt}=F\left(X,Z\right)$$

And we re-write the equation in the infected class as

$$\frac{dZ}{dt} = G(X, Z)$$

Where $X = (S_h, R_h, S_r) \in R^3_+$ denotes the uninfected population and

$Z = (E_h, Q_h, I_h, T_h, E_r, I_r) \in R^6_+$ denotes the infected population

$\eta_0 = (X^*, 0)$ represent the disease free equilibrium of the system, and it is globally asymptotically stable if it satisfies the following conditions [22]:

$H_1 : \frac{dX}{dt} = F(X^*, 0), X^*$ is globally asymptotically stable

$H_2 : \frac{dZ}{dt} = D_Z G(X^*, 0) Z - \hat{G}(X, Z)$

$\hat{G}(X, Z) \geq 0$ for all $(X, Z) \in D$ and where $D_Z G(X^*, 0)$ is an M- matrix, the diagonal elements are non-negative and it is also the Jacobian of $\hat{G}(X, Z) \geq 0$ evaluated at $(X^*, 0)$.

If the system satisfies the above condition, then the theorem below holds.

Theorem 2 [22]

The equilibrium point $\eta_0 = (X^*, 0)$. *is globally asymptotically stable if*

$R_0 \leq 1$, *conditions* H_1 *and* H_2 *are satisfied*

$$F(X, Z) = \begin{bmatrix} \Lambda_h + \sigma_h R_h + \alpha_h Q_h - \frac{(\beta_{rh} I_r + \beta_{hh} I_h) S_h}{N_h} - \mu_h S_h, \\ \psi_h Q_h + \tau_h T_h - (\sigma_h + \mu_h) R_h, \\ \Lambda_r - \frac{\beta_{rr} I_r S_r}{N_r} - \mu_r S_r \end{bmatrix},$$

$$G(X, Z) = \begin{bmatrix} \frac{(\beta_{rh} I_r + \beta_{hh} I_h) S_h}{N_h} - (\omega_h + \theta_h + \mu_h) E_h \\ \omega_h E_h - (\rho_h + \delta_h + \mu_h) I_h \\ \theta_h E_h - (\gamma_h + \mu_h + \delta_h) I_h \\ \theta_h E_h - (\alpha_h + \psi_h + \mu_h) Q_h \\ \rho_h I_h - (\tau_h + \delta_h + \mu_h) T_h \\ \frac{\beta_{rr} I_r S_r}{N_r} - (\omega_r + \mu_r) E_r \\ \omega_r E_r - (\delta_r + \mu_r) I_r \end{bmatrix}$$

At disease free equilibrium,

H_1 :

$$\frac{dS_h}{dt} = \Lambda_h - \mu_h S_h$$
$$\frac{dS_r}{dt} = \Lambda_r - \mu_r S_r$$
$$\frac{dR_h}{dt} = 0$$

H_2 :

$$D_z G(X^*,0)Z = \begin{bmatrix} (\beta_{rh} I_r + \beta_{hh} I_h) - (\omega_h + \theta_h + \mu_h)E_h \\ \omega_h E_h - (\rho_h + \delta_h + \mu_h)I_h \\ \theta_h E_h - (\gamma_h + \mu_h + \delta_h) I_h \\ \theta_h E_h - (\alpha_h + \psi_h + \mu_h)Q_h \\ \rho_h I_h - (\tau_h + \delta_h + \mu_h)T_h \\ \beta_{rr} I_r S_r - (\omega_r + \mu_r)E_r \\ \omega_r E_r - (\delta_r + \mu_r)I_r \end{bmatrix}$$

$$\hat{G}(X,Z) = D_Z G(X^*,0)Z - G(X,Z)$$

$$\hat{G}(X,Z) = \begin{bmatrix} (\beta_{rh} I_r + \beta_{hh} I_h)\left(1 - \frac{S_h}{N_h}\right) \\ 0 \\ 0 \\ 0 \\ \beta_{rr} I_r \left(1 - \frac{S_r}{N_r}\right) \\ 0 \end{bmatrix}$$

Clearly, $1 \geq \frac{S_h}{N_h}, 1 \geq \frac{S_h}{N_h}$ this implies that $\hat{G}(X,Z) \geq 0$.

Therefore, the disease-free equilibrium of the Monkeypox only model is globally asymptotically stable.

2.2 Fractional order of the Monkeypox model

The Caputo derivative is measured as a differential operator in our model. We present in this segment some well-known definitions and effects that we shall be using throughout this research.

Definition 1 The Caputo fractional order derivative of a function (f) on the interval $[O,T]$ is defined by:

$$\left[{}^{C}D_{0}^{\beta}f(t)\right]=\frac{1}{\Gamma(n-\beta)}\int_{0}^{t}(t-s)^{n-\beta-1}f^{(n)}(s)ds, \tag{2}$$

Where $n=[\beta]+1$ and $[\beta]$ represents the integer part of β. In particular, for $0<\beta<1,$ the Caputo derivative becomes:

$$\left[{}^{C}D_{0}^{\beta}f(t)\right]=\frac{1}{\Gamma(1-\beta)}\int_{0}^{t}\frac{f(s)}{(t-s)^{\beta}}ds, \tag{3}$$

Definition 2 Laplace transform of Caputo derivatives is defined as

$$\mathcal{L}[{}^{C}D^{\beta}q(t)]=S^{\beta}h(S)-\sum_{K=0}^{n}S^{\beta-i-1}y^{k}(0),\quad n-1<\beta<n,\ n\in N, \tag{4}$$

For arbitrary $c_i\in R, i=0,1,2,...n-1,\ n=[\beta]+1$ and $[\beta]$ represents the non-integer part of β .

Lemma 1. The following results hold for fractional differentiation equations

$$I^{\beta}[{}^{c}D^{\beta}h](t)=h(t)+\sum_{i=0}^{n-1}\frac{h^{(t)}(0)}{i!}t^{i}, \tag{5}$$

For arbitrary $\beta>0, i=0,1,2,...,n-1,$ where $n=[\beta]+1$ and $[\beta]$ represents the integer part of β Introducing fractional-order into the model, we now present a new model described by the following Introducing fractional order derivative into the model we present new mathematical model describe by set of fractional difference of order β for $0<\beta<1$

$$\left.\begin{aligned}
D^{\beta}\left(S_h\right) &= \Lambda_h + \sigma_h R_h + \alpha_h Q_h - (\mu_h + \lambda_h)s_h,\\
D^{\beta}\left(E_h\right) &= \lambda_h S_h - (\omega_h + \theta_h + \mu_h)E_h,\\
D^{\beta}\left(I_h\right) &= \omega_h E_h - (\rho_h + \delta_h + \mu_h)I_h,\\
D^{\beta}\left(Q_h\right) &= \theta_h E_h - (\alpha_h + \psi_h + \mu_h)Q_h,\\
D^{\beta}\left(T_h\right) &= \rho_h I_h - (\tau_h + \delta_h + \mu_h)T_h,\\
D^{\beta}\left(R_h\right) &= \psi_h Q_h + \tau_h T_h - (\sigma_h + \mu_h)R_h,\\
D^{\beta}\left(S_r\right) &= \Lambda_r - (\mu_r + \lambda_r)S_r,\\
D^{\beta}\left(E_r\right) &= \lambda_r S_r - (\omega_r + \mu_r)E_r,\\
D^{\beta}\left(I_r\right) &= \omega_r E_r - (\delta_r + \mu_r)I_r.
\end{aligned}\right\} \qquad (6)$$

2.3 The Laplace-Adomian Decomposition Method (LADM) Implementation

We considered the general procedure of this method with the initial conditions. Applying Laplace transforms to both sides of the equation (1), and then we have:

$$\left.\begin{aligned}
S^{\beta}\mathcal{L}(S_h) - S^{\beta-1}S_h(0) &= \mathcal{L}\left[\Lambda_h + \sigma_h R_h + \alpha_h Q_h - (\mu_h + \lambda_h)S_h\right]\\
S^{\beta}\mathcal{L}(E_h) - S^{\beta-1}E_h(0) &= \mathcal{L}\left[\lambda_h S_h - (\omega_h + \theta_h + \mu_h)E_h\right]\\
S^{\beta}\mathcal{L}(I_h) - S^{\beta-1}I_h(0) &= \mathcal{L}\left[\omega_h E_h - (\rho_h + \delta_h + \mu_h)I_h\right]\\
S^{\beta}\mathcal{L}(Q_h) - S^{\beta-1}Q_h(0) &= \mathcal{L}\left[\theta_h E_h - (\alpha_h + \psi_h + \mu_h)Q_h\right]\\
S^{\beta}\mathcal{L}(T_h) - S^{\beta-1}T_r(0) &= \mathcal{L}\left[\rho_h I_h - (\tau_h + \delta_h + \mu_h)T_h\right]\\
S^{\beta}\mathcal{L}(R_h) - S^{\beta-1}R_h(0) &= \mathcal{L}\left[\psi_h Q_h + \tau_h T_h - (\sigma_h + \mu_h)R_h\right]\\
S^{\beta}\mathcal{L}(S_r) - S^{\beta-1}S_r(0) &= \mathcal{L}\left[\Lambda_r - (\mu_r + \lambda_r)S_r\right]\\
S^{\beta}\mathcal{L}(E_r) - S^{\beta-1}E_r(0) &= \mathcal{L}\left[\lambda_r S_r - (\omega_r + \mu_r)E_r\right]\\
S^{B}L(I_r) - S^{\beta-1}I_r(0) &= \mathcal{L}\left[\omega_r E_r - (\delta_r + \mu_r)I_r\right]
\end{aligned}\right\} \qquad (7)$$

With initial conditions

$$S_h(0) = n_1,\ \ E_h(0) = n_2,\ I_h(0) = n_3,\ Q_h(0) = n_4,\ T_h(0) = n_5,\ R_h(0) = n_6,\ S_r(0) = n_7,$$

$$E_r(0) = n_8,\ I_r(0) = n_9$$

Dividing eqn. (7) by (S^{β}) we have:

$$\left.\begin{aligned}
\mathcal{L}(S_h) &= \frac{n_1}{S} + \frac{1}{S^{\beta}}\mathcal{L}\left[\Lambda_h + \sigma_h R_h + \alpha_h Q_h - (\mu_h + \lambda_h)S_h\right] \\
\mathcal{L}(E_h) &= \frac{n_2}{S} + \frac{1}{S^{\beta}}\mathcal{L}\left[\lambda_h S_h - (\omega_h + \theta_h + \mu_h)E_h\right] \\
\mathcal{L}(I_h) &= \frac{n_3}{S} + \frac{1}{S^{\beta}}\mathcal{L}\left[\omega_h E_h - (\rho_h + \delta_h + \mu_h)I_h\right] \\
\mathcal{L}(Q_h) &= \frac{n_4}{S} + \frac{1}{S^{\beta}}\mathcal{L}\left[\theta_h E_h - (\alpha_h + \psi_h + \mu_h)Q_h\right] \\
\mathcal{L}(T_h) &= \frac{n_5}{S} + \frac{1}{S^{\beta}}\mathcal{L}\left[\rho_h I_h - (\tau_h + \delta_h + \mu_h)T_h\right] \\
\mathcal{L}(R_h) &= \frac{n_6}{S} + \frac{1}{S^{\beta}}\mathcal{L}\left[\psi_h Q_h + \tau_h T_h - (\sigma_h + \mu_h)R_h\right] \\
\mathcal{L}(S_r) &= \frac{n_7}{S} + \frac{1}{S^{\beta}}\mathcal{L}\left[\Lambda_r - (\mu_r + \lambda_r)S_r\right] \\
\mathcal{L}(E_r) &= \frac{n_8}{S} + \frac{1}{S^{\beta}}\mathcal{L}\left[\lambda_r S_r - (\omega_r + \mu_r)E_r\right] \\
\mathcal{L}(I_r) &= \frac{n_9}{S} + \frac{1}{S^{\beta}}\mathcal{L}\left[\omega_r E_r - (\delta_r + \mu_r)I_r\right]
\end{aligned}\right\} \qquad (8)$$

Decomposing the non-linear term of equation (6) whereby we assume the solution of $S_h(t), E_h(t), I_h(t), Q_h(t), T_h(t), R_r(t), S_r(t), E_r(t), I_r(t)$ are in the form of infinite series given by:

$$S_h(t) = \sum_{n=0}^{\infty} S_h(n), \quad E_h(t) = \sum_{n=0}^{\infty} E_h(n), \quad I_h(t) = \sum_{n=0}^{\infty} I_h(n), \quad Q_h(t) = \sum_{n=0}^{\infty} Q_h(n), \quad T_h(t) = \sum_{n=0}^{\infty} T_h(n),$$
$$R_h(t) = \sum_{n=0}^{\infty} R_h(n), \quad S_r(t) = \sum_{n=0}^{\infty} S_r(n), \quad E_r(t) = \sum_{n=0}^{\infty} E_r(n), \quad I_r(t) = \sum_{n=0}^{\infty} I_r(n), \qquad (9)$$

We have three (5) non-linear terms. The non-linear term in equation (6) are decomposed by Adomian polynomial as follows:

$$I_r(t)S_h(t) = \sum_{n=0}^{\infty} A(n), \qquad I_h(t)S_h(t) = \sum_{n=0}^{\infty} B(n), \qquad I_r(t)S_r(t) = \sum_{n=0}^{\infty} C(n), \tag{10}$$

Where $A(n), B(n), C(n),$ are Adomian polynomials given by

$$A(n) = \frac{1}{\Gamma(n+1)} \frac{d^n}{d\lambda^n} \left[\sum_{k=0}^{n} \lambda^k I_r(k) \sum_{k=0}^{n} \lambda^k S_h(k) \right]_{\lambda=0}$$

$$B(n) = \frac{1}{\Gamma(n+1)} \frac{d^n}{d\lambda^n} \left[\sum_{k=0}^{n} \lambda^k I_h(k) \sum_{k=0}^{n} \lambda^k S_h(k) \right]_{\lambda=0} \tag{11}$$

$$C(n) = \frac{1}{\Gamma(n+1)} \frac{d^n}{d\lambda^n} \left[\sum_{k=0}^{n} \lambda^k I_r(k) \sum_{k=0}^{n} \lambda^k S_r(k) \right]_{\lambda=0}$$

The polynomials are given by

$$\begin{aligned} A(0) &= I_r(0)S_h(0), \\ A(1) &= I_r(0)S_h(1) + I_r(1)S_h(0), \\ A(2) &= I_r(0)S_h(2) + I_r(1)S_h(1) + I_r(2)S_h(0). \end{aligned} \tag{12}$$

$$\begin{aligned} B(0) &= I_h(0)S_h(0), \\ B(1) &= I_h(0)S_h(1) + I_h(1)S_h(0), \\ B(2) &= I_h(0)S_h(2) + I_h(1)S_h(1) + I_h(2)S_h(0). \end{aligned}$$

$$\begin{aligned} C(0) &= I_r(0)S_r(0), \\ C(1) &= I_r(0)S_r(1) + I_r(1)S_r(0), \\ C(2) &= I_r(0)S_r(2) + I_r(1)S_r(1) + I_r(2)S_r(0). \end{aligned}$$

Substituting equation (9), (10) into equation (8) we obtained:

$$
\begin{aligned}
\mathcal{L}\left\{\sum_{n=0}^{\infty} S_h(n)\right\} &= \frac{n_1}{S}+\frac{1}{S^{\beta}}\mathcal{L}\left[\Lambda_h+\sigma_h\sum_{n=0}^{\infty}R_h(n)+\alpha_h\sum_{n=0}^{\infty}Q_h(n)-\left(\frac{\beta_{rh}\sum_{n=0}^{\infty}A(n)+\beta_{hh}\sum_{n=0}^{\infty}B(n)}{N_h}\right)-\mu_h\sum_{n=0}^{\infty}S_h(n)\right]\\
\mathcal{L}\left\{\sum_{n=0}^{\infty} E_h(n)\right\} &= \frac{n_2}{S}+\frac{1}{S^{\beta}}\mathcal{L}\left[\left(\frac{\beta_{rh}\sum_{n=0}^{\infty}A(n)+\beta_{hh}\sum_{n=0}^{\infty}B(n)}{N_h}\right)-\left(\omega_h+\theta_h+\mu_h\right)\sum_{n=0}^{\infty}E_h(n)\right]\\
\mathcal{L}\left\{\sum_{n=0}^{\infty} I_h(n)\right\} &= \frac{n_3}{S}+\frac{1}{S^{\beta}}\mathcal{L}\left[\omega_h\sum_{n=0}^{\infty}E_h(n)-\left(\rho_h+\delta_h+\mu_h\right)\sum_{n=0}^{\infty}I_h(n)\right]\\
\mathcal{L}\left\{\sum_{n=0}^{\infty} Q_h(n)\right\} &= \frac{n_4}{S}+\frac{1}{S^{\beta}}\mathcal{L}\left[\theta_h\sum_{n=0}^{\infty}E_h(n)-(\alpha_h+\psi_h+\mu_h)\sum_{n=0}^{\infty}Q_h(n)\right]\\
\mathcal{L}\left\{\sum_{n=0}^{\infty} T_h(n)\right\} &= \frac{n_5}{S}+\frac{1}{S^{\beta}}\mathcal{L}\left[\rho_h\sum_{n=0}^{\infty}Q_h(n)-(\tau_h+\delta_h+\mu_h)\sum_{n=0}^{\infty}T_h(n)\right]\\
\mathcal{L}\left\{\sum_{n=0}^{\infty} R_h(n)\right\} &= \frac{n_6}{S}+\frac{1}{S^{\beta}}\mathcal{L}\left[\psi_h\sum_{n=0}^{\infty}Q_h(n)+\tau_h\sum_{n=0}^{\infty}T_h(n)-(\sigma_h+\mu_h)\sum_{n=0}^{\infty}R_h(n)\right]\\
\mathcal{L}\left\{\sum_{n=0}^{\infty} S_r(n)\right\} &= \frac{n_7}{S}+\frac{1}{S^{\beta}}\mathcal{L}\left[\Lambda_r-\frac{\beta_{rr}\sum_{n=0}^{\infty}C(n)}{N_r}-\mu_r\sum_{n=0}^{\infty}S_r(n)\right]\\
\mathcal{L}\left\{\sum_{n=0}^{\infty} E_r(n)\right\} &= \frac{n_8}{S}+\frac{1}{S^{\beta}}\mathcal{L}\left[\frac{\beta_{rr}\sum_{n=0}^{\infty}C(n)}{N_r}-(\omega_r+\mu_r)\sum_{n=0}^{\infty}E_r(n)\right]\\
\mathcal{L}\left\{\sum_{n=0}^{\infty} I_r(n)\right\} &= \frac{n_9}{S}+\frac{1}{S^{\beta}}\mathcal{L}\left[\omega_r\sum_{n=0}^{\infty}E_r(n)-(\delta_r+\mu_r)\sum_{n=0}^{\infty}I_r(n)\right]
\end{aligned}
\tag{13}
$$

Evaluating the Laplace transform of the 2nd terms in the RHS of (16), we obtain

$$
\begin{aligned}
\mathcal{L}\left\{\sum_{n=0}^{\infty} S_h(n)\right\} &= \frac{n_1}{S} + \left[\Lambda_h + \sigma_h \sum_{n=0}^{\infty} R_h(n) + \alpha_h \sum_{n=0}^{\infty} Q_h(n) - \left(\frac{\beta_{rh} \sum_{n=0}^{\infty} A(n) + \beta_{hh} \sum_{n=0}^{\infty} B(n)}{N_h}\right) - \mu_h \sum_{n=0}^{\infty} S_h(n)\right] \frac{1}{S^{\beta+1}} \\
\mathcal{L}\left\{\sum_{n=0}^{\infty} E_h(n)\right\} &= \frac{n_2}{S} + \left[\left(\frac{\beta_{rh} \sum_{n=0}^{\infty} A(n) + \beta_{hh} \sum_{n=0}^{\infty} B(n)}{N_h}\right) - \left(\omega_h + \theta_h + \mu_h\right) \sum_{n=0}^{\infty} E_h(n)\right] \frac{1}{S^{\beta+1}} \\
\mathcal{L}\left\{\sum_{n=0}^{\infty} I_h(n)\right\} &= \frac{n_3}{S} + \left[\omega_h \sum_{n=0}^{\infty} E_h(n) - \left(\rho_h + \delta_h + \mu_h\right) \sum_{n=0}^{\infty} I_h(n)\right] \frac{1}{S^{\beta+1}} \\
\mathcal{L}\left\{\sum_{n=0}^{\infty} Q_h(n)\right\} &= \frac{n_4}{S} + \left[\theta_h \sum_{n=0}^{\infty} E_h(n) - (\alpha_h + \psi_h + \mu_h) \sum_{n=0}^{\infty} Q_h(n)\right] \frac{1}{S^{\beta+1}} \\
\mathcal{L}\left\{\sum_{n=0}^{\infty} T_h(n)\right\} &= \frac{n_5}{S} + \left[\rho_h \sum_{n=0}^{\infty} Q_h(n) - (\tau_h + \delta_h + \mu_h) \sum_{n=0}^{\infty} T_h(n)\right] \frac{1}{S^{\beta+1}} \\
\mathcal{L}\left\{\sum_{n=0}^{\infty} R_h(n)\right\} &= \frac{n_6}{S} + \left[\psi_h \sum_{n=0}^{\infty} Q_h(n) + \tau_h \sum_{n=0}^{\infty} T_h(n) - (\sigma_h + \mu_h) \sum_{n=0}^{\infty} R_h(n)\right] \frac{1}{S^{\beta+1}} \\
\mathcal{L}\left\{\sum_{n=0}^{\infty} S_r(n)\right\} &= \frac{n_7}{S} + \left[\Lambda_r - \frac{\beta_{rr} \sum_{n=0}^{\infty} C(n)}{N_r} - \mu_r \sum_{n=0}^{\infty} S_r(n)\right] \frac{1}{S^{\beta+1}} \\
\mathcal{L}\left\{\sum_{n=0}^{\infty} E_r(n)\right\} &= \frac{n_8}{S} + \left[\frac{\beta_{rr} \sum_{n=0}^{\infty} C(n)}{N_r} - (\omega_r + \mu_r) \sum_{n=0}^{\infty} E_r(n)\right] \frac{1}{S^{\beta+1}} \\
\mathcal{L}\left\{\sum_{n=0}^{\infty} I_r(n)\right\} &= \frac{n9}{S} + \left[\omega_r \sum_{n=0}^{\infty} E_r(n) - (\delta_r + \mu_r) \sum_{n=0}^{\infty} I_r(n)\right] \frac{1}{S^{\beta+1}}
\end{aligned}
\tag{14}
$$

Taking the inverse Laplace transform of both sides of (14)

$$\left.\begin{aligned}
\sum_{n=0}^{\infty} S_h(n) &= n_1 + \left[\Lambda_h + \sigma_h \sum_{n=0}^{\infty} R_h(n) + \alpha_h \sum_{n=0}^{\infty} Q_h(n) - \left(\frac{\beta_{rh} \sum_{n=0}^{\infty} A(n) + \beta_{hh} \sum_{n=0}^{\infty} B(n)}{N_h}\right) - \mu_h \sum_{n=0}^{\infty} S_h(n)\right] \frac{t^{\beta}}{\Gamma(\beta+1)} \\
\sum_{n=0}^{\infty} E_h(n) &= n_2 + \left[\left(\frac{\beta_{rh} \sum_{n=0}^{\infty} A(n) + \beta_{hh} \sum_{n=0}^{\infty} B(n)}{N_h}\right) - \left(\omega_h + \theta_h + \mu_h\right) \sum_{n=0}^{\infty} E_h(n)\right] \frac{t^{\beta}}{\Gamma(\beta+1)} \\
\sum_{n=0}^{\infty} I_h(n) &= n_3 + \left[\omega_h \sum_{n=0}^{\infty} E_h(n) - \left(\rho_h + \delta_h + \mu_h\right) \sum_{n=0}^{\infty} I_h(n)\right] \frac{t^{\beta}}{\Gamma(\beta+1)} \\
\sum_{n=0}^{\infty} Q_h(n) &= n_4 + \left[\theta_h \sum_{n=0}^{\infty} E_h(n) - (\alpha_h + \psi_h + \mu_h) \sum_{n=0}^{\infty} Q_h(n)\right] \frac{t^{\beta}}{\Gamma(\beta+1)} \\
\sum_{n=0}^{\infty} T_h(n) &= n_5 + \left[\rho_h \sum_{n=0}^{\infty} Q_h(n) - (\tau_h + \delta_h + \mu_h) \sum_{n=0}^{\infty} T_h(n)\right] \frac{t^{\beta}}{\Gamma(\beta+1)} \\
\sum_{n=0}^{\infty} R_h(n) &= n_6 + \left[\psi_h \sum_{n=0}^{\infty} Q_h(n) + \tau_h \sum_{n=0}^{\infty} T_h(n) - (\sigma_h + \mu_h) \sum_{n=0}^{\infty} R_h(n)\right] \frac{t^{\beta}}{\Gamma(\beta+1)} \\
\sum_{n=0}^{\infty} S_r(n) &= n_7 + \left[\Lambda_r - \frac{\beta_{rr} \sum_{n=0}^{\infty} C(n)}{N_r} - \mu_r \sum_{n=0}^{\infty} S_r(n)\right] \frac{t^{\beta}}{\Gamma(\beta+1)} \\
\sum_{n=0}^{\infty} E_r(n) &= n_8 + \left[\frac{\beta_{rr} \sum_{n=0}^{\infty} C(n)}{N_r} - (\omega_r + \mu_r) \sum_{n=0}^{\infty} E_r(n)\right] \frac{t^{\beta}}{\Gamma(\beta+1)} \\
\sum_{n=0}^{\infty} I_r(n) &= n_9 + \left[\omega_r \sum_{n=0}^{\infty} E_r(n) - (\delta_r + \mu_r) \sum_{n=0}^{\infty} I_r(n)\right] \frac{t^{\beta}}{\Gamma(\beta+1)}
\end{aligned}\right\} \quad (15)$$

When $n=0$ we obtain,

$$S_h(0) = n_1,\ \ E_h(0) = n_2,\ I_h(0) = n_3,\ Q_h(0) = n_4,\ T_h(0) = n_5,\ R_h(0) = n_6,\ S_r(0) = n_7,$$

$$E_r(0) = n_8,\ I_r(0) = n_9 \quad (16)$$

When $n=1$, we obtain,

$$
\left.
\begin{aligned}
S_h(1) &= \left[\Lambda_h + \sigma_h R_h(0) + \alpha_h Q_h(0) - \left(\frac{\beta_{rh} A(0) + \beta_{hh} B(0)}{N_h} \right) - \mu_h S_h(0) \right] \frac{t^\beta}{\Gamma(\beta+1)} \\
E_h(1) &= \left[\left(\frac{\beta_{rh} A(0) + \beta_{hh} B(0)}{N_h} \right) - \left(\omega_h + \theta_h + \mu_h \right) E_h(0) \right] \frac{t^\beta}{\Gamma(\beta+1)} \\
I_h(1) &= \left[\omega_h E_h(0) - \left(\rho_h + \delta_h + \mu_h \right) I_h(0) \right] \frac{t^\beta}{\Gamma(\beta+1)} \\
Q_h(1) &= \left[\theta_h E_h(0) - (\alpha_h + \psi_h + \mu_h) Q_h(0) \right] \frac{t^\beta}{\Gamma(\beta+1)} \\
T_h(1) &= \left[\rho_h Q_h(0) - (\tau_h + \delta_h + \mu_h) \mathrm{T}_h(0) \right] \frac{t^\beta}{\Gamma(\beta+1)} \\
R_h(1) &= \left[\psi_h Q_h(0) + \tau_h T_h(1) - (\sigma_h + \mu_h) R_h(0) \right] \frac{t^\beta}{\Gamma(\beta+1)} \\
S_r(1) &= \left[\Lambda_r - \frac{\beta_{rr} C(0)}{N_r} - \mu_r S_r(0) \right] \frac{t^\beta}{\Gamma(\beta+1)} \\
E_r(1) &= \left[\frac{\beta_{rr} C(0)}{N_r} - (\omega_r + \mu_r) E_r(0) \right] \frac{t^\beta}{\Gamma(\beta+1)} \\
I_r(1) &= \left[\omega_r E_r(0) - (\delta_r + \mu_r) I_r(0) \right] \frac{t^\beta}{\Gamma(\beta+1)}
\end{aligned}
\right\} \quad (17)
$$

When $n = 2$, we obtain,

$$
\left.
\begin{aligned}
S_h(2) &= \left[\Lambda_h + \sigma_h R_h(1) + \alpha_h Q_h(1) - \left(\frac{\beta_{rh} A(1) + \beta_{hh} B(1)}{N_h} \right) - \mu_h S_h(1) \right] \frac{t^\beta}{\Gamma(\beta+1)} \\
E_h(2) &= \left[\left(\frac{\beta_{rh} A(1) + \beta_{hh} B(1)}{N_h} \right) - \left(\omega_h + \theta_h + \mu_h \right) E_h(1) \right] \frac{t^\beta}{\Gamma(\beta+1)} \\
I_h(2) &= \left[\omega_h E_h(1) - \left(\rho_h + \delta_h + \mu_h \right) I_h(1) \right] \frac{t^\beta}{\Gamma(\beta+1)} \\
Q_h(2) &= \left[\theta_h E_h(1) - (\alpha_h + \psi_h + \mu_h) Q_h(1) \right] \frac{t^\beta}{\Gamma(\beta+1)} \\
T_h(2) &= \left[\rho_h Q_h(1) - (\tau_h + \delta_h + \mu_h) \mathrm{T}_h(1) \right] \frac{t^\beta}{\Gamma(\beta+1)} \\
R_h(2) &= \left[\psi_h Q_h(1) + \tau_h T_h(1) - (\sigma_h + \mu_h) R_h(1) \right] \frac{t^\beta}{\Gamma(\beta+1)} \\
S_r(2) &= \left[\Lambda_r - \frac{\beta_{rr} C(1)}{N_r} - \mu_r S_r(1) \right] \frac{t^\beta}{\Gamma(\beta+1)} \\
E_r(2) &= \left[\frac{\beta_{rr} C(1)}{N_r} - (\omega_r + \mu_r) E_r(1) \right] \frac{t^\beta}{\Gamma(\beta+1)} \\
I_r(2) &= \left[\omega_r E_r(1) - (\delta_r + \mu_r) I_r(1) \right] \frac{t^\beta}{\Gamma(\beta+1)}
\end{aligned}
\right\} \quad (18)
$$

When $n = n+1$, we obtain,

$$
\left.
\begin{aligned}
S_h(n+1) &= \left[\Lambda_h + \sigma_h R_h(n) + \alpha_h Q_h(n) - \left(\frac{\beta_{rh} A(n) + \beta_{hh} B(n)}{N_h} \right) - \mu_h S_h(n) \right] \frac{t^\beta}{\Gamma(\beta+1)} \\
E_h(n+1) &= \left[\left(\frac{\beta_{rh} A(n) + \beta_{hh} B(n)}{N_h} \right) - \left(\omega_h + \theta_h + \mu_h \right) E_h(n) \right] \frac{t^\beta}{\Gamma(\beta+1)} \\
I_h(n+1) &= \left[\omega_h E_h(n) - \left(\rho_h + \delta_h + \mu_h \right) I_h(n) \right] \frac{t^\beta}{\Gamma(\beta+1)} \\
Q_h(n+1) &= \left[\theta_h E_h(n) - (\alpha_h + \psi_h + \mu_h) Q_h(n) \right] \frac{t^\beta}{\Gamma(\beta+1)} \\
T_h(n+1) &= \left[\rho_h Q_h(n) - (\tau_h + \delta_h + \mu_h) \mathrm{T}_h(n) \right] \frac{t^\beta}{\Gamma(\beta+1)} \\
R_h(n+1) &= \left[\psi_h Q_h(n) + \tau_h T_h(1) - (\sigma_h + \mu_h) R_h(n) \right] \frac{t^\beta}{\Gamma(\beta+1)} \\
S_r(n+1) &= \left[\Lambda_r - \frac{\beta_{rr} C(n)}{N_r} - \mu_r S_r(n) \right] \frac{t^\beta}{\Gamma(\beta+1)} \\
E_r(n+1) &= \left[\frac{\beta_{rr} C(n)}{N_r} - (\omega_r + \mu_r) E_r(n) \right] \frac{t^\beta}{\Gamma(\beta+1)} \\
I_r(n+1) &= \left[\omega_r E_r(n) - (\delta_r + \mu_r) I_r(n) \right] \frac{t^\beta}{\Gamma(\beta+1)}
\end{aligned}
\right\} \quad (19)
$$

The series solution of each compartment can be expressed as:

$$
\begin{aligned}
S_h(t) &= S_h(0) + S_h(1) + S_h(2) + \ldots \\
E_h(t) &= E_h(0) + E_h(1) + E_h(2) + \ldots \\
I_h(t) &= I_h(0) + I_h(1) + I_h(2) + \ldots \\
Q_h(t) &= Q_h(0) + Q_h(1) + Q_h(2) + \ldots \\
T_h(t) &= T_h(0) + T_h(1) + T_h(2) + \ldots \\
R_h(t) &= R_h(0) + R_h(1) + R_h(2) + \ldots \\
S_r(t) &= S_r(0) + S_r(1) + S_r(2) + \ldots
\end{aligned}
\quad (20)
$$

$$E_r(t) = E_r(0) + E_r(1) + E_r(2) + \ldots$$

$$I_r(t) = I_r(0) + I_r(1) + I_r(2) + \ldots$$

2.5 Numerical solution of Laplace Adomian Decomposition Method (LADM)

Numerical simulation plays a key role in mathematical epidemiology, allowing researchers to model and explore how diseases spread within populations. These models are often built on systems of differential equations that represent important factors, such as infection and recovery rates, as well as patterns of movement within the population. By solving these equations over time, simulations can forecast how a disease may progress under different conditions. Additionally, numerical simulations help in estimating parameters and analyzing sensitivity within epidemiological models [20]. Parameter estimation involves matching model outputs with real-world data to determine key values, like transmission rates or initial conditions, while sensitivity analysis examines how changes in these parameters impact the model's predictions. This approach helps ensure that the predictions are reliable and provides insights into which factors most influence disease spread. Simulations also allow researchers to test various scenarios and intervention strategies, such as the effects of vaccination programs, social distancing, or healthcare capacity changes on disease dynamics [22]. This makes simulation a critical tool for guiding public health responses and policies, offering valuable support for planning interventions during outbreaks. Overall, numerical simulations are essential for deepening our understanding of disease dynamics, shaping effective public health strategies, and preparing for future epidemics.

Therefore, we conduct the numerical solution of the model using the initial conditions and parameter values in MATLAB, the Laplace Adomian Decomposition Method (LADM) gives us an approximate solution in in terms of an infinite series presented as:

$$\left.\begin{aligned}
S_h(t) &= 30000 - 350.97\frac{t^{\beta}}{\Gamma(\beta+1)} - 524.37\frac{t^{2\beta}}{\Gamma(2\beta+1)} + \ldots \\
E_h(t) &= 10000 - 208.64\frac{t^{\beta}}{\Gamma(\beta+1)} + 5142.89\frac{t^{2\beta}}{\Gamma(2\beta+1)} + \ldots \\
I_h(t) &= 7000 + 252.41\frac{t^{\beta}}{\Gamma(\beta+1)} - 3656.46\frac{t^{2\beta}}{\Gamma(2\beta+1)} + \ldots \\
Q_h(t) &= 5000 + 164.37\frac{t^{\beta}}{\Gamma(\beta+1)} + 175.37\frac{t^{2\beta}}{\Gamma(2\beta+1)} + \ldots \\
T_h(t) &= 4500 - 309.92\frac{t^{\beta}}{\Gamma(\beta+1)} - 798800\frac{t^{2\beta}}{\Gamma(2\beta+1)} + \ldots \\
R_h(t) &= 4000 - 544.13\frac{t^{\beta}}{\Gamma(\beta+1)} - 798850\frac{t^{2\beta}}{\Gamma(2\beta+1)} + \ldots \\
S_r(t) &= 6000 - 104.53\frac{t^{\beta}}{\Gamma(\beta+1)} - 1.66\frac{t^{2\beta}}{\Gamma(2\beta+1)} + \ldots \\
E_r(t) &= 3000 - 16.09\frac{t^{\beta}}{\Gamma(\beta+1)} - 3.19\frac{t^{2\beta}}{\Gamma(2\beta+1)} + \ldots \\
I_r(t) &= 1500 - 327.38\frac{t^{\beta}}{\Gamma(\beta+1)} + 149.01\frac{t^{2\beta}}{\Gamma(2\beta+1)} + \ldots
\end{aligned}\right\} \quad (21)$$

For $\beta = 1$, the series solution of our model becomes,

$$\left.\begin{aligned}
S_h(t) &= 200000 - 429.97t - 262.185t^2 + \ldots \\
E_h(t) &= 150000 - 25080.46t + 2571.445t^2 + \ldots \\
I_h(t) &= 13000 + 25298.11t - 1828.23t^2 + \ldots \\
Q_h(t) &= 9000 + 168.73t + 87.685t^2 + \ldots \\
T_h(t) &= 10000 - 419.29t - 399400t^2 + \ldots \\
R_h(t) &= 8000 - 466.31t + 3991425t^2 + \ldots \\
S_r(t) &= 9000 - 194.35t - 0.834t^2 + \ldots \\
E_r(t) &= 10000 - 12.49t - 1.595t^2 + \ldots \\
I_r(t) &= 8000 - 1427.93t + 129.51t^2 + \ldots
\end{aligned}\right\} \quad (22)$$

Table 2. **Parameter Values used in the Model**

Parameters	Value	Sources
Λ_h	0.029	Assumed
Λ_r	0.9	Assumed
β_{rh}	0.00025	[19]
β_{hh}	0.00006	[20]
β_{rr}	0.027	[20]
ω_h	0.07	Assumed
ρ_h	0.002	[20]
θ_h	0.2	[20]
μ_r	0.00200	Assumed
τ_h	0.02	[20]
α_h	0.0001	[17]
σ_h	0.00001	Assumed
δ_h	0.02	[20]
δ_r	0.5	[18]
μ_h	0.05	Assumed
ω_r	0.007	Assumed

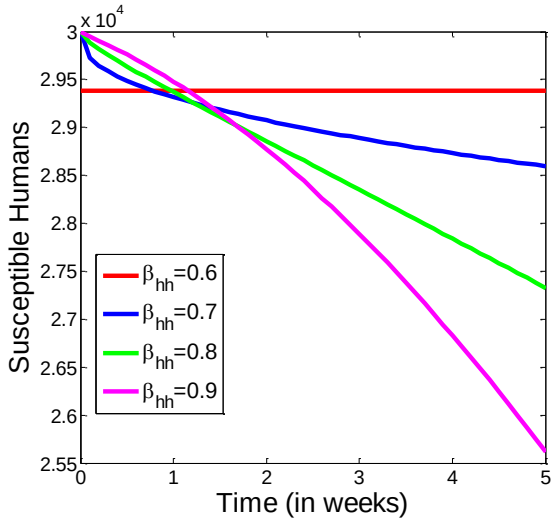

Figure 2a: Graph of susceptible humans

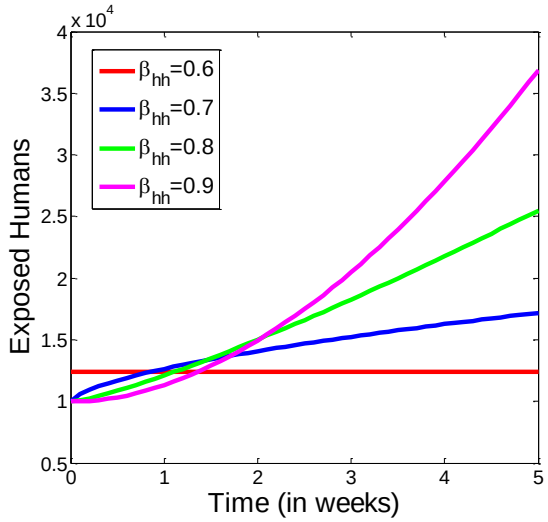

Figure 2b: Graph of Exposed humans

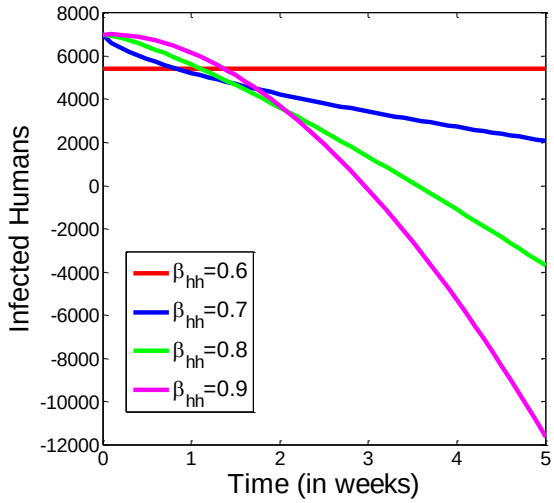

Figure 2c: Graph of infected humans humans

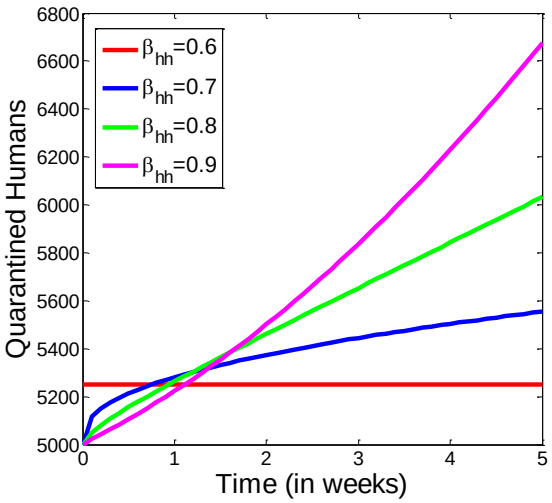

Figure 2d: Graph of quarantined

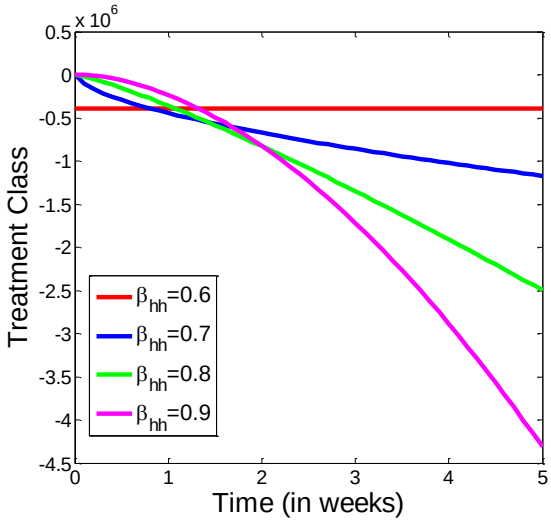

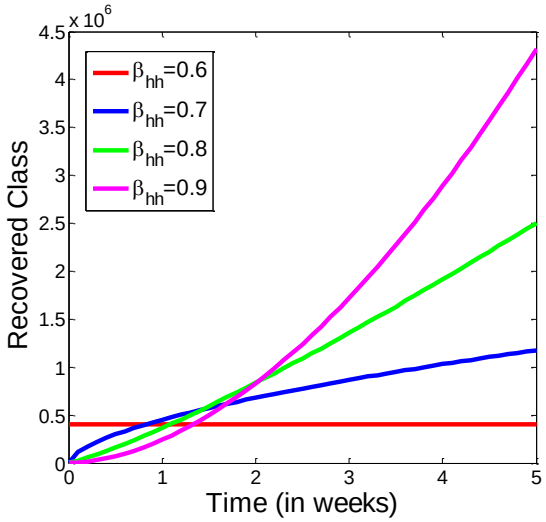

Figure 2e: Graph of treatment classFigure 2f: Graph of recovered humans

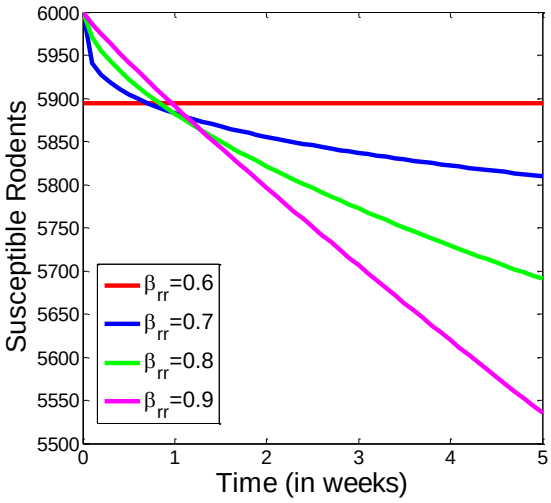

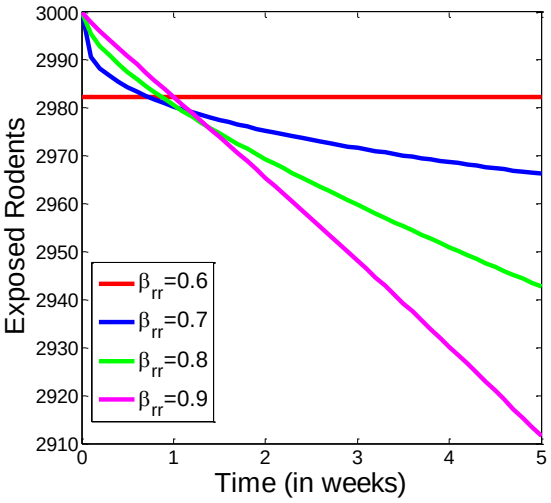

Figure 2g: Graph of susceptible rodents Figure 2h: Graph of Exposed rodents

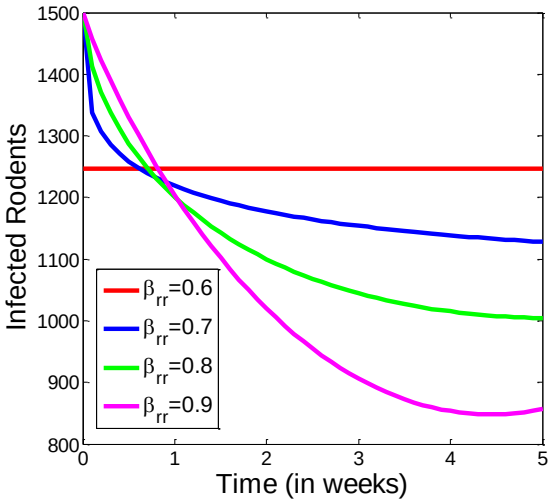

Figure 2i: Graph of infected rodents

In Figure 2a, we observe a steady decline in the graph of susceptible humans over time. This trend suggests effective control of the monkeypox virus, as fewer individuals within the population remain susceptible. This decrease implies that, eventually, almost no new cases are likely to emerge as the susceptible population approaches zero. However, Figure 2b shows an initial increase in the number of exposed humans. This rise occurs as susceptible individuals become exposed to the virus before prevention measures take full effect. After this initial increase, the exposed population also declines, indicating that interventions reduce the risk of exposure over time. In Figure 2c, the number of infected humans decreases steadily. This decline is likely due to effective quarantine measures, as shown in Figure 2d. Quarantine helps prevent the virus from spreading among the population by isolating infected individuals. As a result, the number of humans requiring treatment, illustrated in Figure 2e, also decreases. This decrease in active treatment cases is a promising sign, as it aligns with the observed high recovery rate in Figure 2f. Together, these trends suggest that both treatment and quarantine measures are effectively managing human cases of monkeypox, leading to an increase in recovered individuals. In Figure 2g, the graph of susceptible rodents also shows a significant decline over time. This trend indicates that control measures are not only effective for humans but are also helping reduce the number of susceptible rodents, which play a role in the transmission cycle. Figure 2h mirrors this effect in the exposed rodent population. Initially, there may be an increase in exposed rodents, but over time, the number of exposed rodents decreases as the virus is brought under control in their population as well. Finally, Figure 2i illustrates a complete decline in the number of infected rodents, eventually reaching zero. This result is a clear indicator of successful disease control. By eliminating the rodent population as a reservoir for the virus, the likelihood of further outbreaks decreases significantly, pointing to effective measures in controlling monkeypox transmission within both human and rodent populations.

3. Convergence analysis for the Laplace-Adomian Decomposition Method (LADM).

The solution of (1) is expressed in the forms of infinite series which converged uniformly to its exact solution. To verify the convergence of the series (21), we employ the method used in [18]. For sufficient conditions of convergence of the LADM, we present the following theorem:

Theorem 1

Let X be a Banach space and $T: X \to X$ *be a constructive nonlinear operator such that for* $(x),(x)' \in X,\ \left\|T(x)-T(x')\right\|, 0<k<1.$ *Then, T has a unique point x such that* $Tx = x$ *,where* $x = (S_H, E_H, I_H, R_H, S_M, E_M, I_M, S_W, E_W, I_W)$. *The series given () can be written by applying the Adomian decomposition method as follows:*

$$x_n = Tx_{n-1}, x_{n-1},$$

$$= \sum_{i=1}^{n-1} x_i,\ n = 1,2,3,...$$

And we assume that $x_0 \in B_r(x)$, *where* $B_r(x) = \left\{x \in X : \left\|x' - x\right\| < r\right\}$; *then, we have as follows:*

(i) $x_n \in B_r(x)$

(ii) $\lim_{n\to\infty} x_n = x$

Proof

For condition (i), invoking mathematical induction,

For n=1, we have as follows:

$$\left\|x_0 - x\right\| = \left\|T(x_0) - T(x)\right\| \le \left\|x_0 - x\right\|.$$

If this is true for m-1, then

$$\left\|x_0 - x\right\| \le k^{m-1}\left\|x_0 - x\right\|.$$

This gives the following:

$$\left\|x_m - x\right\| = \left\|T(x_{m-1}) - T(x)\right\| \le k\left\|x_{m-1} - x\right\| \le k^n\left\|x_0 - x\right\|.$$

Therefore,

$$\|x_m - x\| \leq k^n \|x_0 - x\| \leq k^n r < r.$$

This directly implies that $x_n \in B_r(x)$.

Also, for (ii), we have that since $\|x_m - x\| \leq k^n \|x_0 - x\|$ and $\lim_{n\to\infty} k^n = 0$, we can write $\lim_{n\to\infty} x_n = x$.

4 Conclusion

Our research presents a practical model for understanding how monkeypox spreads between humans and rodents, highlighting key strategies to control the disease. The results show that reducing the number of susceptible humans over time, combined with measures like quarantining and treating those infected, is highly effective in limiting the spread of monkeypox among people. In the rodent population, reducing the number of both susceptible and exposed animals plays an essential role in minimizing overall infection risks for humans. By using the Laplace Adomian Decomposition Method, we were able to predict how the disease would likely behave under different public health strategies. Our findings emphasize the importance of quickly isolating infected individuals, providing timely treatment, and managing rodent populations to reduce potential sources of infection. This model offers valuable insights for public health planning, suggesting that a comprehensive approach targeting both human and rodent populations is essential to controlling monkeypox. This framework could be adapted for similar zoonotic diseases, providing a basis for developing proactive strategies to prevent outbreaks and protect public health.

References

[1] World Health Organization (2022) . https://www.who.int/europe/news-room/23-07-2022-who-director-general-declares-the-ongoing-monkeypox-outbreak-a-public-health-event-of-international-concern

[2] CDC. (2023). Epidemiologic and clinical features of mpox-associated deaths in the United States. Retrieved from https://www.cdc.gov.

[3] Frontiers. (2023). Insights into monkeypox pathophysiology, global prevalence, clinical manifestation, and treatments. Retrieved from https://www.frontiersin.org

[4] Abdelrahman, M. M., & El-Sayed, A. M. (2020). Application of Laplace-Adomian Decomposition Method for solving some epidemiological models. Mathematics and Computers in Simulation, 173, 35-43.

[5] Chowdhury, M. S. H., Hamid, M. A., & Rahman, M. M. (2021). Analytical solution of SEIR model of infectious disease by using Laplace Adomian Decomposition Method. Results in Applied Mathematics, 10, 100168.

[6] Kanth, A. R., & Arshad, M. (2018). The use of Laplace Adomian Decomposition Method in solving biological models. Journal of Applied Mathematics and Physics, 6(4), 743-751.

[7] Kaya, D., & Cimen, S. (2015). A comparative analysis of Adomian Decomposition and Laplace-Adomian Decomposition Methods. Computers & Mathematics with Applications, 70(7), 1453-1461.
[8] Singh, J., & Kumar, M. (2019). Laplace-Adomian Decomposition Method for solving nonlinear problems. International Journal of Mathematical Analysis and Applications, 6(4), 15-21.
[9] Brauer, F., Castillo-Chavez, C., & Feng, Z. (2019). Mathematical Models in Epidemiology. New York: Springer.
[10] Kucharski, A. J., Russell, T. W., Diamond, C., Liu, Y., Edmunds, J., Funk, S., & Eggo, R. M. (2020). Early dynamics of transmission and control of COVID-19: A mathematical modelling study. The Lancet Infectious Diseases, 20(5), 553-558.
[11] Vynnycky, E., & White, R. (2018). An Introduction to Infectious Disease Modelling. Oxford University Press.
[12] Endo, A., Murayama, H., Abbott, S., Ratnayake, R., Pearson, C. A. B., Edmunds, W. J., & Funk, S. (2022). Estimating the reproduction number of monkeypox in non-endemic countries. Eurosurveillance, 27(22), 2200486.
[13] Grant, R., Hayes, S., Pybus, O. G., & Frost, S. D. (2023). Evaluating vaccination strategies against monkeypox transmission in the UK. Journal of Infectious Diseases, 227(3), 1024-1033.
[14] Yinka-Ogunleye, A., Aruna, O., Dalhat, M., Ogoina, D., McCollum, A. M., & Nkomo, P. (2022). Modeling zoonotic and human-to-human transmission of monkeypox in West Africa. Tropical Medicine & International Health, 27(4), 451-459.
[15] Al-Najjar, H., Al-Azzam, M., Al-Dabbas, B., & Mansour, A. (2023). Impact of behavior change on monkeypox transmission: A dynamic modeling approach. *Computational and Mathematical Methods in Medicine, 2023, 375162.
[16] Hebert-Dufresne, L., Althouse, B. M., Scarpino, S. V., & Allard, A. (2022). Network-based modeling of monkeypox transmission in social and sexual networks. Epidemics, 38, 100527.
[17] Agbata, B. C., Odeh, O. J., Anni, B. N., Odo, C. E., & Olorunnishola, O. A. (2019). Mathematical assessment of the transmission dynamics of HIV/AIDS with treatment as control effects. International Journal of Mathematics and Statistics Studies, 7(4), 40-52.
[18] Agbata, B. C., Shior, M. M., Obeng-Denteh, W., Omotehinwa, T. O., Paul, R. V., Kwabi, P. A., & Asante-Mensa, F. (2023). A mathematical model of COVID-19 transmission dynamics with effects of awareness and vaccination program. Journal of Global Scientific Academy, 21(2), 59-61.
[19] Odeh, J. O., Agbata, B. C., Ezeafulukwe, A. U., Madubueze, C. E., Acheneje, G. O., & Topman, N. N. (2024). A mathematical model for the control of chlamydia disease with treatment strategy. Journal of Mathematical Analysis and Research, 7(1), 1-20.
[20] Olumuyiwa, J. P., Sumit, K., Nitu, K., Festus, A. O., Kayode, O., & Rabiu, M. (2021). Transmission dynamics of monkeypox virus: A mathematical modeling approach. Modeling Earth System and Environment. https://dio.org/10.1007/s40808-021-013313-2
[21] Agbata, B.C., Obeng-Denteh, W., Amoah-Mensah, J. Kwabi, P.A., Shior, M.M., Asante Mensa, F, Abraham, S (2024). Numerical solution of fractional order model of measles disease with double dose vaccination. DUJOPAS. 10(3b): 202-217
[22] Agbata, B.C, Obeng-Denteh, W, Raimonda Dervish, Kwabi P.A., Habeed A. Aal-Rkhais, Asente-Mensa, F Ezugorie I.G, Arivi S.S. (2024). Mathematical modeling and analysis of Monkeypox transmission dynamics with treatment and quarantine interventions. *DUJOPAS*, 10 (4b): 78-96
[23] Somma, S. A., Akinwande, N. I., & Chado, U. D. (2019). A mathematical model of monkeypox virus transmission dynamics. Ife Journal of Science, 21(1), 195–204.

[24] Castillo-Chavez, C., & Song, B. (2004). Mathematical models of epidemics. *Mathematical Biosciences, 188*(2), 35-58. https://doi.org/10.1016/j.mbs.2004.03.005Malaria is a very deadly disease, which has taken a toll on human activities [1]. As seen in [2,3], evidences abound as to the source of the latest epidemic.